Virchows Archiv (1994) 424:477–484

ORIGINAL ARTICLE

Yasumitsu Okouchi · Katsunori Sasaki · Tohru Tamaki

Ultrastructural changes in hepatocytes, sinusoidal endothelial cells and macrophages in hypothermic preservation of the rat liver with University of Wisconsin solution

Received: 16 November 1993 / Accepted: 3 March 1994

Abstract To identify subtle changes which might lead to liver failure after liver transplantation, rat livers stored at 4° C in University of Wisconsin solution for 8, 16, 24, and 32 h were examined by transmission electron microscopy, scanning electron microscopy, cellular matrix maceration and freeze fracture for ultrastructural analysis. Endothelial cells exhibited aggregation of intramembrane particles (IMPs) at 8 h and produced tiny blebs accompanied by marked development of pits. As deterioration advanced, endothelial cells exposed the perisinusoidal faces of hepatocytes directly to the lumen with destruction of sieve plates. They then degraded with loss of IMPs. Macrophages followed a similar deterioration process to endothelial cells. Membranes of hepatocytes did not demonstrate aggregations of IMPs for 32 h. Rough endoplasmic reticulum (rER) lost ribosomes and smooth ER (sER) increased in amount and dilated in an irregular form. Autophagosomes appeared in the cytoplasm, engulfed cytoplasmic matrix containing intracellular organelles and became autophagic vacuoles. At 32 h bile canaliculi were filled with detached vesicles. This may be one of the causes of preservation related bile duct complications after liver transplantation.

Key words Liver · Tissue preservation · Bleb
Intramembrane particles · Autophagocytosis

Y. Okouchi (✉)
Department of Surgery, Shimada Memorial Hospital,
607-22 Fujioka, Gunma 375, Japan

K. Sasaki
Department of Anatomy, Yokohama City University
School of Medicine, 3-9 Fukuura, Kanazawa-ku, Yokohama 236, Japan

T. Tamaki
Department of Organ Transplantation, Hachioji Medical Centre,
1163 Tatemachi, Hachioji, Tokyo 193, Japan

Introduction

University of Wisconsin (UW) solution was introduced in the field of organ preservation for transplantation in 1986 [44] and has a clear advantage over Euro-Collins solution, a previously widely used kidney and liver preservation fluid [16, 27]. UW solution is also used in tissue preparation for electron microscopy [41].

Sinusoidal endothelial cells are considered to be more sensitive to cold ischaemia than hepatocytes [26] and the ultrastructure of hepatocytes is well maintained for 48 h storage with UW solution [27]. Bleb formation is one of the major ultrastructural changes seen in the sinusoid of preserved liver, and occurs mainly in hepatocytes [26, 28, 29]. Why blebs are formed on ultrastructurally well maintained hepatocytes is unknown. In this study, we examined movement of intramembrane particle by freeze fracture, transmission electron microscopy (TEM), scanning EM (SEM), and matrix cell maceration method during liver storage with UW solution in order to indentify subtle changes which might lead to liver failure after liver transplantation.

Materials and methods

Female Wistar rats aged 9–11 weeks were obtained from Sankyo Labo Service Company, Japan. All animals received humane care in compliance with "Guide for the care and use of laboratory animals" published by National Institutes of Health (publication number 86–23, revised 1985). Diet and water were fed ad libitum before experimentation. The anaesthesia and procedure for liver procurement were similar to that for a donor operation of rat liver transplantation [31], except that subhepatic inferior vena cava, common bile duct, and phrenic vein were not prepared. Rat livers were perfused with cold UW solution through portal vein and preserved in the same solution at 4° C for 0, 8, 16, 24, or 32 h before fixation. Eight and 32 h time points were chosen because these are survival and nonsurvival points in the rat liver transplantation model and they are the main time points currently studied. The whole liver was perfusion fixed at each time point, and the left lobe was used for the study. One of the components of UW solution, hydroxyethyl starch, was a gift from Green Cross Company, Japan.

For TEM rat livers were examined at 0(n=3), 8(n=3), 16(n=2), 24(n=2) and 32(n=3) h. Three to four samples were studied from each liver. The cold-stored livers were perfused and fixed with 2% glutaraldehyde in cacodylate buffer solution (0.08 M, pH 7.3). A part of the left lateral lobe was excised, cut into small pieces and immersed in the same fixation solution for 1 h. The pieces were then washed with cacodylate buffer, postfixed with 1% osmium tetroxide (OsO_4) in cacodylate buffer solution for 1 h, dehydrated in an ethanol series and embedded in Polybed/Araldite mixture. Ultra-thin and semi-thin sections were prepared with an ultramicrotome (Ultracut N, Reichert-Jung, Austria) and ultra-thin sections were stained with uranyl acetate and lead citrate and examined with a JEM 2000EX electron microscope (JOEL, Japan).

For SEM rat livers were examined at 0(n=3), 8(n=3), 16(n=2), 24(n=2) and 32(n=3) h. Five samples were studied from each liver. The liver was perfused, fixed and cut in the same way as for TEM. The samples were then fixed with 2% glutaraldehyde in cacodylate buffer for 1 h and postfixed with 1% OsO_4 for 2 h. They were then immersed in 70% ethanol for 10 min. The ethanol was changed three times. The samples were then frozen on the aluminum plate which had been cooled by liquid nitrogen and were fractured by a razor blade. They were then transferred into 70% ethanol and dehydrated in an ethanol series. Dehydrated samples were immersed in isoamyl acetate for more than 3 h, dried with a HCP-2 critical point drying device (Hitachi, Japan), and then coated with 20 nm thickness of platinum-gold using a SC500 sputter coater (Emscope, UK). Samples were observed with a S-800 SEM (Hitachi).

The cellular matrix maceration method [39] was used to observe intracellular structures by SEM. Rat livers were examined at 0(n=2), 8(n=2) and 32(n=2) h. Five samples were studied from each liver. The livers were perfused with 70 ml of cacodylate buffer solution then 30 ml of 2% glutaraldehyde for 2 min and flushed again with 30 ml of buffer solution. The samples were postfixed in 1% OsO_4 at 4° C for 2 h, then transferred into 70% ethanol and exchanged three times for 10 min each. The tissues were then frozen on an aluminum plate chilled with liquid nitrogen and cracked by a razor blade. The samples were brought back into 70% ethanol, kept for 10 min at room temperature, rinsed with two changes of buffer solution, and macerated in 0.1% OsO_4 for 4 h at room temperature. After that, they were dehydrated in an ethanol series and followed the above method for SEM.

In freeze-fracture studies livers were examined at 0(n=3), 8(n=3), 16(n=2), 24(n=2) and 32(n=3) h. Three samples were studied from each liver. After perfusion fixation with 2% glutaraldehyde cacodylate buffer solution and washing with buffer solution, the samples were immersed in 25% glycerol in cacodylate buffer from 1 to 1.5 h then transferred to specimen-holders, frozen in liquid freon and quickly transferred to a freeze-fracture device (BAF 301, Balzers, Switzerland). They were fractured at a stage temperature of −130° C. The fractured surface was shadowed with platinum-carbon evaporated from an electron beam gun at a 45° angle, and the carbon was then evaporated at a 90° angle. The tissues were digested with perchloric acid for a minimum of 3 h. After washing, the replicas were placed on copper grids and observed with the EM.

Results

In the membranous plane of normal hepatocytes, numerous intramembrane particles (IMPs) were distributed uniformly (Fig. 1a). Hepatocytes were sealed by tight

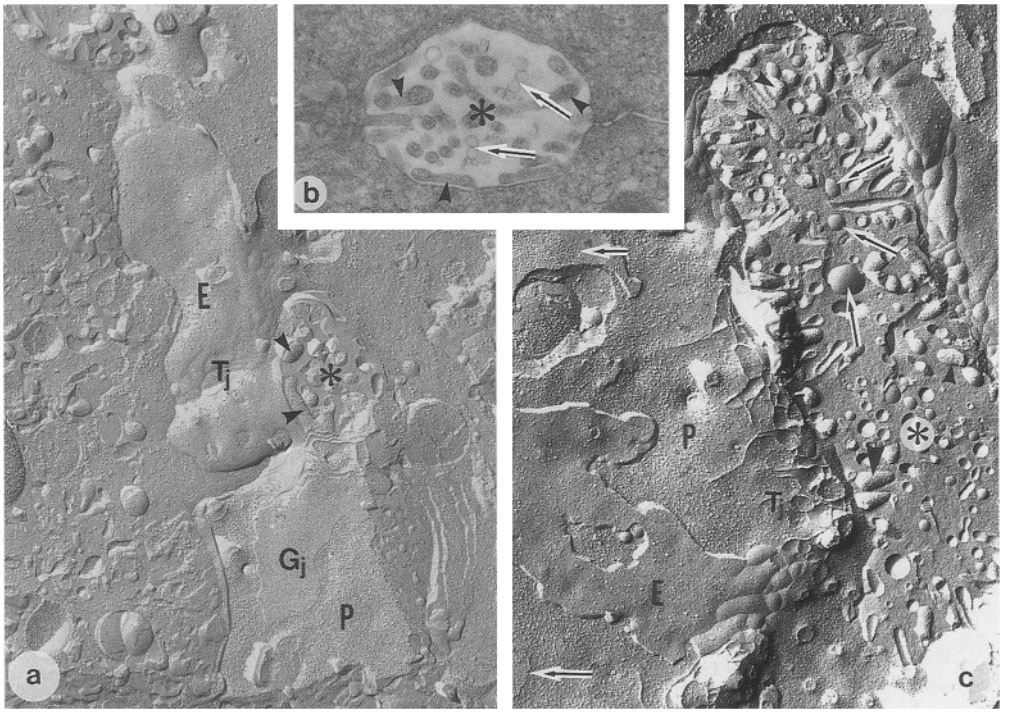

Fig. 1a–c Hepatocyates. Cytoplasmic membrane and bile canaliculi. **a** A replica of normal hepatocytes. Intramembrane particles (IMPs) in the protoplasmic (*P*) and exoplasmic (*E*) faces were distributed homogeneously. Gap junctions (*Gj*) and tight junctions (*Tj*) develop well. The fracture planes of cytoplasmic processes (*arrowheads*) in the bile canaliculi (*asterisk*) possess numerous and uniformly distributed IMPs. × 22,000. **b** Ultra-thin section of a bile canaliculus (*asterisk*) stored in UW solution for 32 h. The tips of cytoplasmic processes (*arrowheads*) are swollen. Small vesicles (*arrows*) are detached in the canaliculi. These vesicles are very low in electron density, varied in size and continuous like beads. × 22,000. **c** A replica of hepatocytes at 32 h preservation. IMPs of *E* and *P* faces are distributed homogeneously, respectively, although number of particles seem to decrease slightly. *Tj* and *Gj* (*short arrows*) remain intact. The replica of a bile canaliculus (*asterisk*) is featured by bulging tips of cytoplasmic processes (*arrowheads*) and many vesicles of varying sizes (*arrows*) without IMPs. These features are comparable to those in (**b**). × 25,000

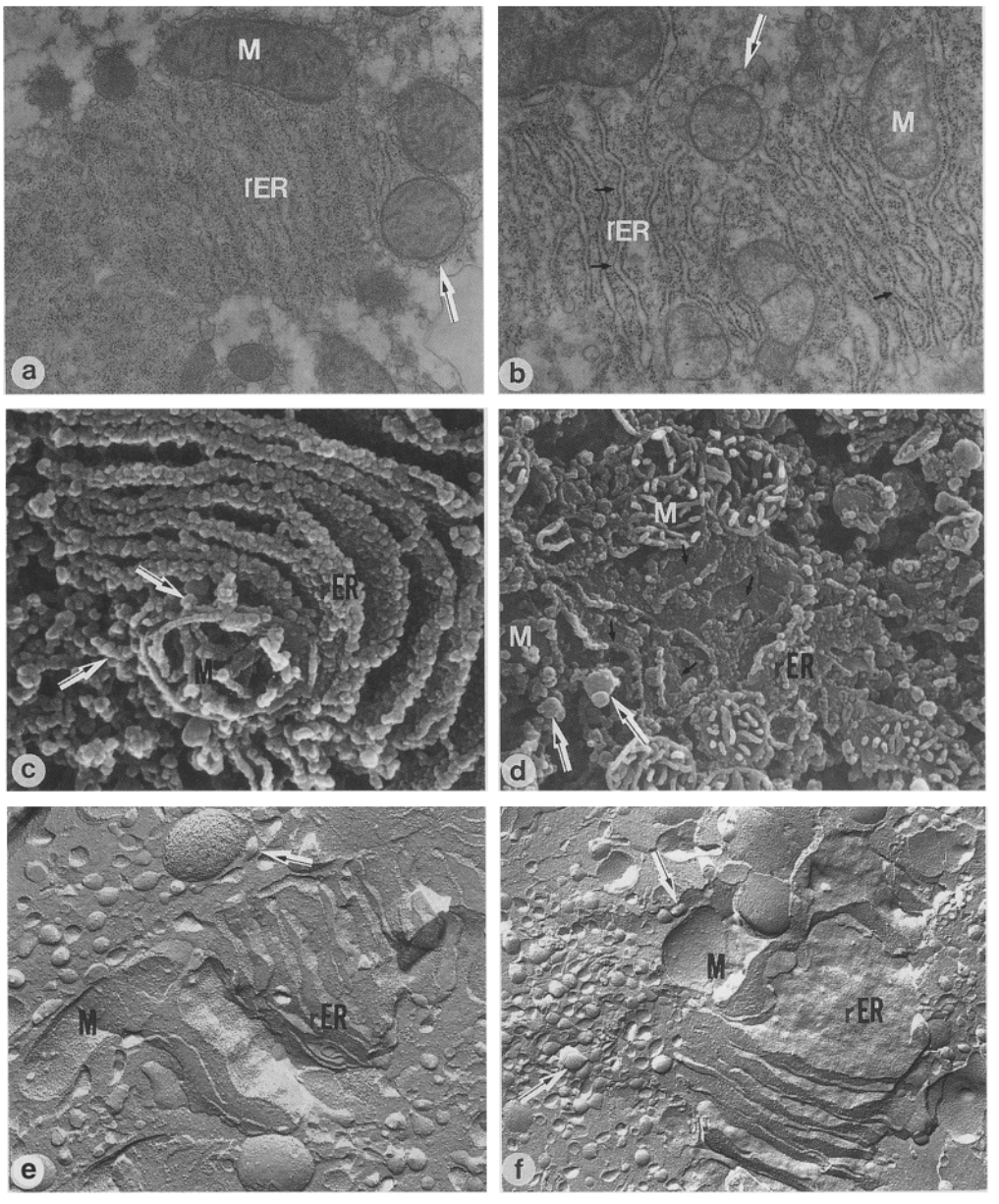

Fig. 2a–f Hepatocytes Intracellular organelles [mitochondria (*M*), rough endoplasmic reticulum (*rER*), and smooth endoplasmic reticulum (*sER*)]. **a** *M*, *rER* and sER in a normal hepatocyte. *sER* surrounds a mitochondrion like a chain (*arrow*). × 18,000 **b** *M*, *rER* and sER at 32 h preservation. *rER* loses ribosomes in places (*short arrows*). sER in the vicinity of a *M* takes vesicular forms (*arrow*) with larger diameter than normal. × 22,000. **c** *rER* and sER and *M* in a normal hepatocyte observed by scanning electron microscopy (SEM) after removal of cellular matrix. *rER* possesses rich ribosomes. sER (*arrows*) attaching to the outer surface of a mitochondrion is continuous with peripheral sER network. × 73,000. **d** *rER* and *M* at 32 h preservation. *rER* shows nude areas (*short arrows*) containing no ribosomes. Spherical vesicles with large size than usual sER are in the vicinity of a *M*. × 51,000. **e** A replica of *rER* and sER and *M* of normal hepatocytes. IMPs in these organelle are distributed homogeneously. An arrow shows sER surrounding a *M*. × 22,000. **f** A replica of *rER* and sER and *M* at 32 h preservation. IMPs in the fracture plane of *rER* and *M* did not aggregate. sER increases near *rER* and takes vesicular forms (*arrows*) with varied sizes. Compare with Fig. 3 (**a**) × 18,000

junctions formed along a bile canaliculus. Gap junctions extended and developed well on the hepatocellular surface. No aggregation of IMPs was observed for 32 h (Fig. 1c). At 32 h IMPs seemed to be more sparse and bile canaliculi showed marked degradative alterations. Microprocesses in bile canaliculi swelled at the tip (Fig. 1b, c). Small vesicles, which filled the lumen, seemed to originate from cytoplasmic processes and were frequently continuous like beads and did not possess IMPs in freeze replica. Though intracellular organelles of hepatocytes did not present aggregations of IMPs for 32 h, their ultrastructure showed deterioration. Rough endoplasmic reticulum (rER) lost ribosomes (Fig. 2a–d) at 32 h. In normal hepatocytes, smooth ER (sER) surrounded mitochondria like a chain (Fig. 2a, c) but at 32 h sER was increased, dilated and seemed to be pinched off as irregular vesicles (Fig. 2b, d, f). The formation of autophagosomes was specific to hepatocytes and appeared in an incomplete manner at 8 h (Fig. 3). A few linear structures were seen in ultra-thin sections, these were frequently lamellar, segregated near rich sER regions (Fig. 3a) and were identified as smooth membranous structures by SEM (Fig. 3b). Later membranes engulfed part of the cytoplasm containing mitochondria and sER to form autophagosomes (Fig. 3c, d). In freeze fracture, these phagosomes had lost IMPs in most parts of the membrane except for small regions with particle aggregations. The autophagosomes gave rise to autophagic vacuoles containing vesicles and a part of cytoplasmic matrix (Fig. 4a, b). Membranes fractured in a complicated pattern (Fig. 4c) and did not exhibit aggregations of IMPs.

Significant features of sinusoidal endothelial cells during cold storage were small blebs, pit formation, and

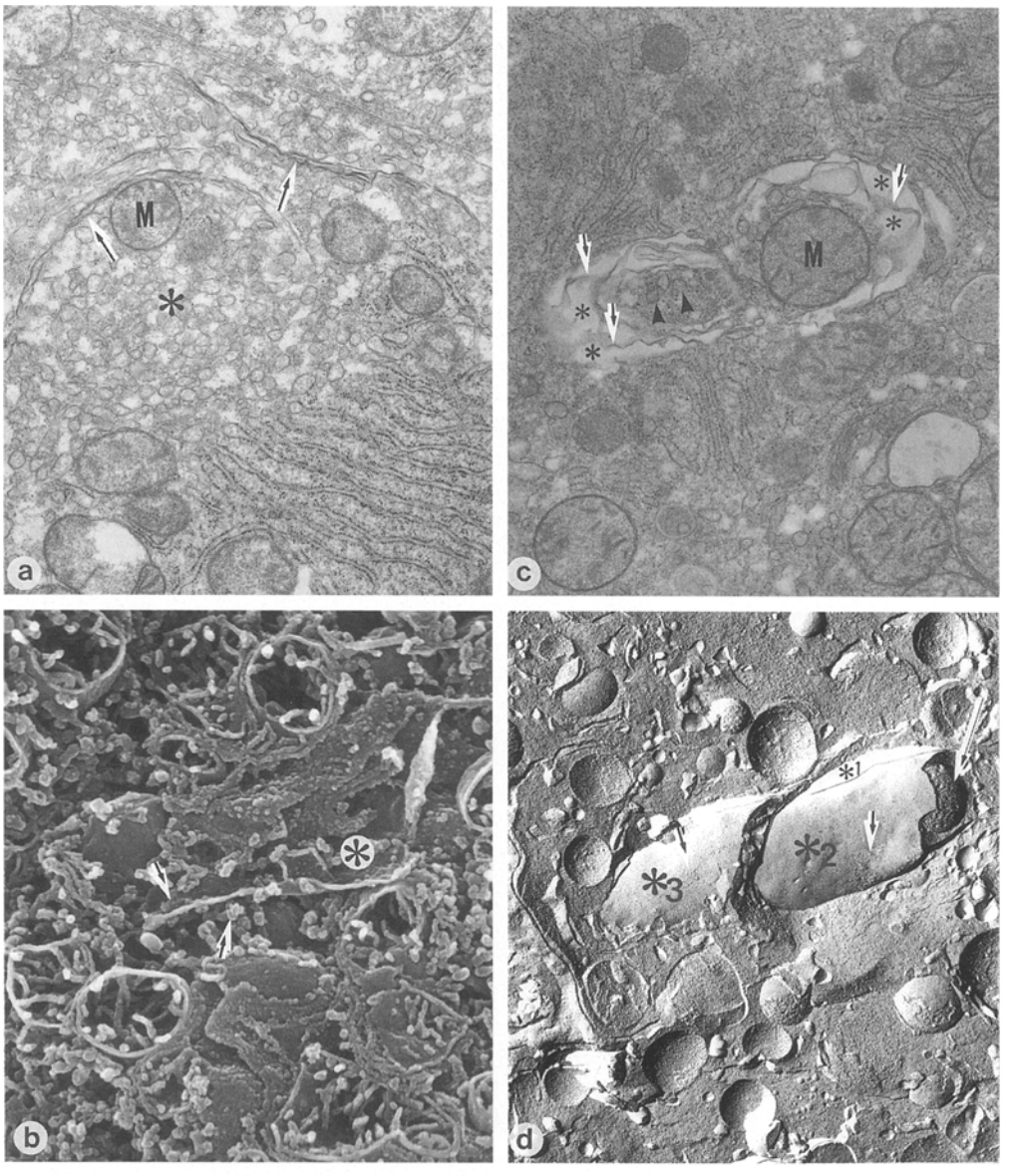

Fig. 3a–d Hepatocytes. Formation of autophagosomes. **a** Thin section of a hepatocyte at 8 h. Dilated sER (*asterisk*) with more irregular diameters increases markedly. Linear structures (*arrows*) close to the dilated sER segregate, which seems to be continuous with sER. *M* contacts their inner part. These are the beginning of formation of autophagosomes. × 19,000. **b** SEM at 32 h shows that these linear structures are membranous (*asterisk*), which have few particles on the surface and are associated with sER (*arrows*). × 41,000. **c** Mature autophagosomes at 24 h. Strands (*arrows*) extend from the periphery towards the central area containing vesicles (*arrowheads*) and *M* and form spaces (*asterisks*). × 20,000. **d** A replica of autophagosomes at 16 h. An autophagosome is fractured lamellarly (*asterisks 1 and 2*). In the fracture face, IMPs aggregate partly (*arrows*), but are almost lost extensively (*asterisks 1, 2, 3*). Crossing fracture of phagosomal matrix contains a *M* (*long arrow*). × 17,000

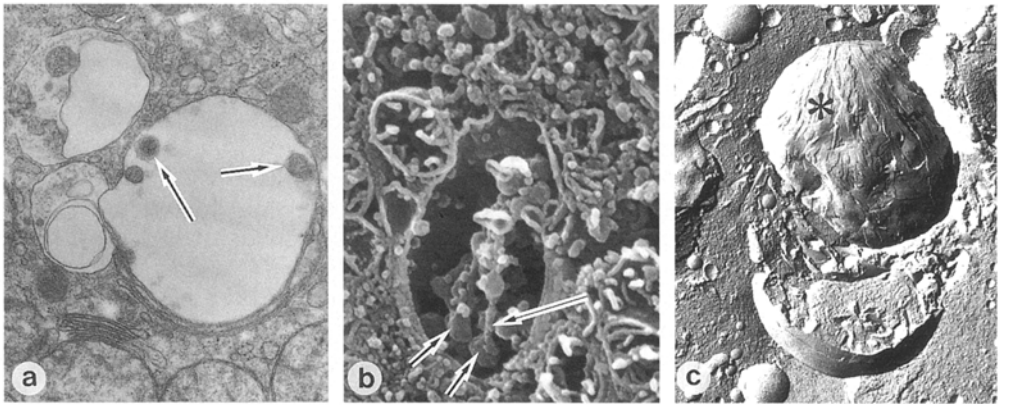

Fig. 4a–c Hepatocytes. Autophagic vacuoles. **a** Ultra-thin section shows a vacuole in a hepatocyte at 24 h including granules (*arrows*) with high density. × 22,000. **b** SEM demonstrates granules (*arrows*) and interconnecting strands (*long arrow*) between them in a vacuole at 32 h. × 37,000. **c** A fracture face of vacuoles at 8 h exhibits complicated, lamellar structures (*asterisk*). × 17,000

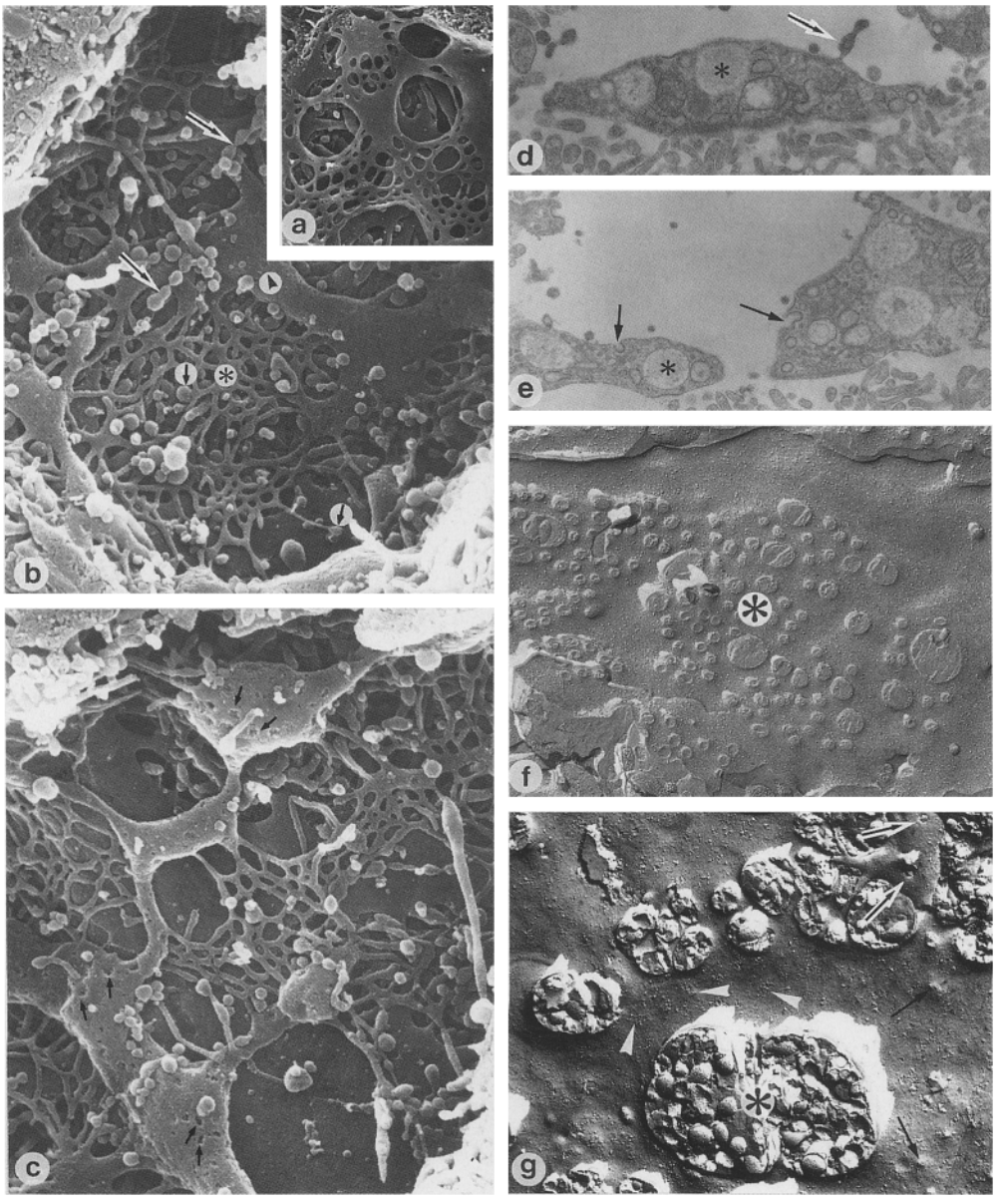

Fig. 5a–g Hepatic sinusoidal endothelial cell. **a** A normal structure of a sinusoidal lumen disclosing smooth surface and typical sieve plates. × 20,000. **b** At 8 h the surface of endothelial cell is rough. The structure of sieve plates (*asterisk*) becomes mesh-like. Sieve plates are interrupted in places, where broken tips inflate (*short arrows*). Many vesicles stick to the areas. They are single or form bead-like structures (*long arrows*). Small irregular pits are identified in the cell body (*arrowhead*). × 30,000. **c** The endothelial cell at 16 h preservation. Irregular dilatations of sieve plate are found here and there and some of the sieve plates are lost. Defects (*arrows*) in the cell body surface increase. × 30,000. **d** Ultra-thin section of endothelial cells at 8 h preservation proves that some blebs (*arrow*) connect to a cell body. Blebs rarely originate from hepatic cells. The matrix of endothelial cells increase in density. The cytoplasm contains many vacuoles (*asterisk*). × 14,000. **e** Endothelial cells at 8 h preservation. Pits (*arrows*) develop well. Two pits fuse and become large ones. They correspond to the defects seen in SEM (**b, c**). × 23,000. **f** A replica of normal endothelial cells. IMPs are distributed homogeneously. Sieve plates (*asterisk*) are recognized as areas consisting of varied-size circles. × 23,000. **g** A replica of an endothelial cell at 16 h. IMPs aggregate (*white arrowheads*). Small protuberants (*arrows*) are seen. They are counterparts to defects in **b, c** and pits in **e**. An *asterisk* shows a sieve plate, in which many microvilli of a hepatocyte are exposed. × 17,000

change of surface texture in the luminal surface. The surface of normal endothelial cells was smooth and formed sieve plates associated with fenestration (Fig. 5a). The discrete cytoplasm among small fenestrae was slender. At 8 h, a large number of tiny blebs appeared on endothelial cells and sieve plates (Fig. 5b). Some of them seemed to be derived from microvilli, but many were apparently derived from endothelial cells. Their diameters ranged from 0.05 to 0.2 mm and their size remained the same. They were single or bead-like. The slender cytoplasm forming the fenestrae swelled in the middle or was broken to bulge at the tips. Small irregular pits were formed in the cell body at 8 h (Fig. 5b) and were marked at 16 h (Fig. 5c). Ultra-thin section showed that many of these small blebs originated from endothelial cells (Fig. 5d). Pits in another section of endothelial cell developed well and fused to form more complicated and larger ones (Fig. 5e). Though IMPs in normal endothelial cells were distributed homogeneously (Fig. 5f), they aggregated in small groups in places at 8 h (Fig. 5g). Prolonged preservation caused hepatocytes to produce large blebs in the perisinusoidal surfaces as well as in the hepatocellular surfaces at 32 h (Fig. 6a, b).

The pattern of deterioration of macrophages was similar to that of endothelial cells. Macrophages formed tiny blebs like those seen in endothelial cells in the surface at 8 h (Fig. 6c, d). A few of them seemed to be connected to the surface (Fig. 6c). Though IMPs in the membranous plane of normal macrophages were distributed uniformly and depressions were moderate in number (Fig. 6e), IMPs aggregated at 8 h and many depressions with varied sizes were formed (Fig. 6d, e). At 16 h, a macrophage exhibited a large giant swelling of cytoplasm containing no intracellular organelles, which was like a larger bleb seen in hepatocytes (Fig. 6f). At the final stage,

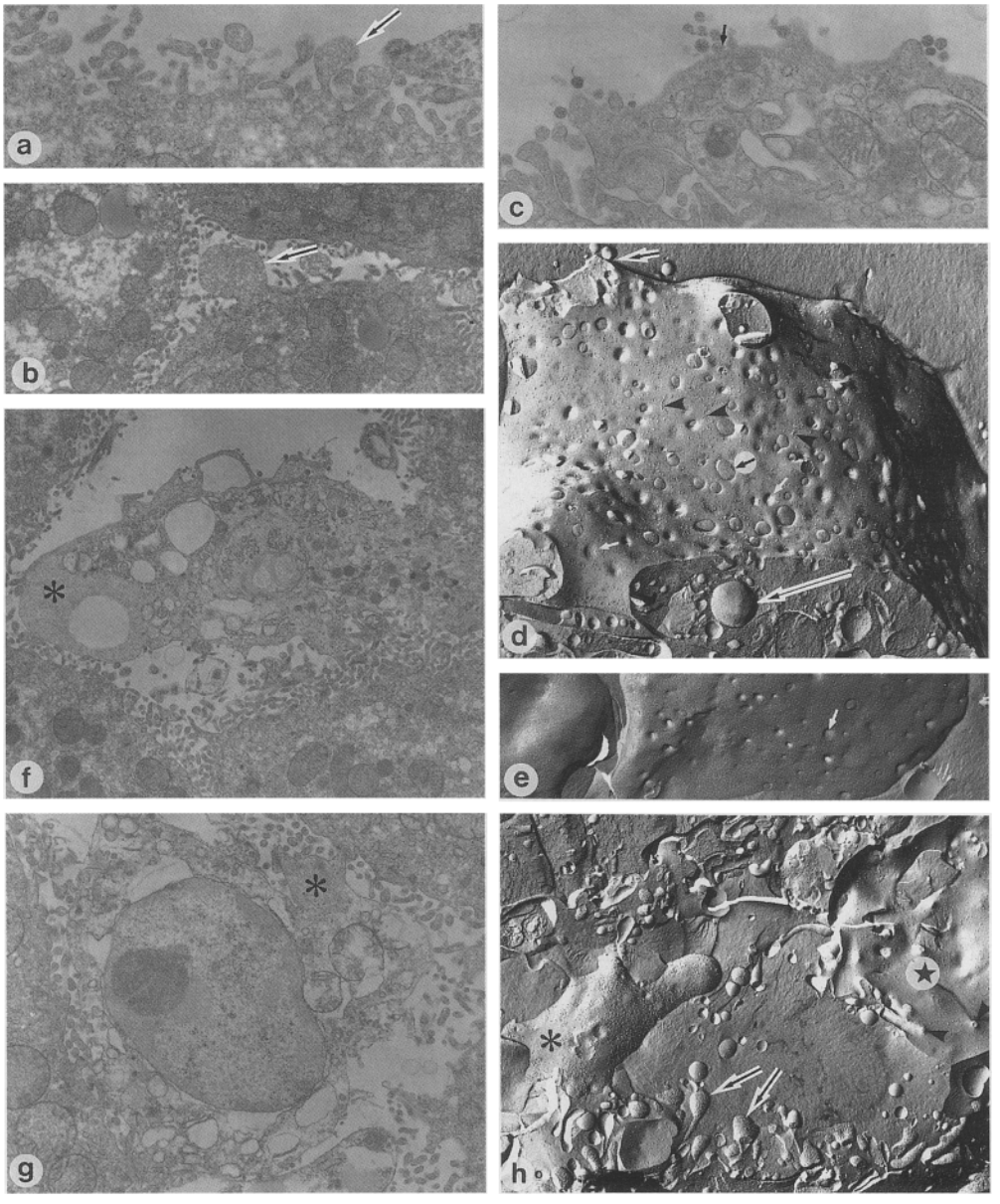

Fig. 6a–h Bleb formation of hepatocytes and fate of macrophage. **a** Blebs (*arrow*) originating from hepatocyte are typically formed in surfaces facing the hepatic sinusoid at 32 h. They inflate at the tips of microvilli. Before this stage, bleb formation can rarely be identified in hepatocytes. × 13,000. **b** Blebs (*arrow*) are formed in the hepatocellular surface of hepatocytes and detached in the separate space (*asterisk*). × 6,000. **c** At 8 h a macrophage formed many small blebs (*arrow*) with high electron density, which are similar to small blebs seen in endothelial cell and appear to be continuous with macrophages. At least macrophages do not engulf them. × 15,000. **d** A replica of a macrophage at 8 h. Intramembrane particles aggregate like strands (*arrowheads*). Small depressions develop well (*white arrows*). Large circular depressions (*short arrow in the white circle*) are also observed. Vesicles (*short arrow*) attach to the surface. In a replica the connection of vesicles to the surface of the macrophage can not be confirmed. A vacuole (*long arrow*) in the cytoplasm loses IMPs. × 16,000. **e** A replica of a normal macrophage. Comparing to **d**, IMPs are distributed evenly, the size of depressions (*white arrow*) is uniform and less in number. Large depressions are not conspicuous. × 11,000. **f** Ultra-thin section of a macrophage at 8 h shows dramatic changes of the cytoplasm. Vacuoles, secondary lysosomes and residual bodies increase markedly. The specific cytoplasmic swelling (*asterisk*) containing no intracellular organelles develops in the periphery. It is similar to the blebs of hepatocytes seen in **b**. × 6,000. **g** The final stage of macrophage at 24 h. The matrix is lost and vacuoles increase. Membranes of the cytoplasm and organelles are interrupted in places. The cytoplasm protrudes irregularly like a bleb (*asterisk*). × 10,000. **h** A replica of macrophages and microvilli of hepatocytes at 32 h. Particle-free areas and aggregations of IMPs intermingle in the *P* face of a macrophage (*asterisk*). *Arrows* show replicas of blebs formed in hepatocytes. The particles are lost partly. The E face of the macrophage (*star*) discloses subtle deficiency of membrane particles and small projections of coated pits (*arrowheads*). × 1,200

macrophages lost their cytoplasmic matrix, mitochondria, and IMPs and formed many vacuoles and interrupted membranes (Fig. 6g, h).

Discussion

IMPs are considered to be composed of various transmembrane proteins. Redistribution of IMPs is caused by various conditions such as hypothermia [11], ischaemia [6, 13], activation of platelets [7] and other factors [40], and is considered to be a sign of deterioration [36]. The redistribution of IMPs caused by hypothermia is interpreted as a result of lateral phase separation in the plasma membrane [35]. Lateral phase separation may result in increased permeability of the membrane and is considered to be harmful, although probably reversible. Redistribution of IMPs caused by ischaemia is considered to be caused by loss of phospholipids or binding of calcium ions to lipids of membrane, both resulting in decreased membrane fluidity [13]. The aggregation of IMPs during renal ischaemia is reversible if the ischaemia time is short, later becoming irreversible [6] and should thus be considered an early sign of injury. During simple cold storage, the liver is exposed to hypothermia and ischaemia combined but aggregation of IMPs is not found in the plasma membrane of hepatocyte at 32 h. However, aggregation of IMPs is obvious in sinusoidal endothelial cells and macrophages at 8 h, demonstrating the relative resistance of hepatocytes to hypothermic injury. The redistribution of IMPs in endothelium is related to marked pit formation, clearly demonstrated with TEM and replica. Pinocytosis is supposedly associated with the movement of IMPs [33].

One of the characteristic morphological changes during liver preservation is the formation of blebs [18]. Blebbing is an early consequence of hypoxic injury to cells, and may eventually cause death of the cell [24]. It may occur in apoptosis [42]. Blebbing is also observed during hypoxia in other organs including the proximal convoluted tubule of the kidney [8] and cerebal endothelium [5, 25]. Blebs may be shed [19, 23] and cause circulatory disturbance [28]; large blebs may narrow sinusoidal lumina and cause death after transplantation. Blebs formed following hypothermic liver preservation [26, 27, 29], or hypoxia [22, 23] are considered to originate from hepatocytes. In our study, there were two kinds of blebs, small (0.05–0.2 mm) and large (several mm). Small blebs were mainly derived from endothelial cells and were conspicuous at 8 h. They had high electron density and sometimes formed bead-like structures. As blebs may cause reduction of cell volume [12], the numerous small blebs seen might reduce cell volume producing mesh-like changes in endothelial cells and exposing the sinusoidal surfaces of hepatocytes. The blebs formed on isolated hepatocytes are reversible at early stages of hypoxia [17] and the small endothelial blebs may also be reversible since 8 h-preserved liver is capable of supporting life after transplantation [32]. These surface changes could be mechanical obstacles for passage of leucocytes which has been shown to be delayed after hypothermic preservation [43]. We saw no large blebs on endothelial cells before their death but these appeared on the perisinusoidal and hepatocellular surfaces of hepatocyles after 24 h

Blebs are also formed on bile canalicular surfaces of hepatocytes, probably because bile canaliculi may not be exposed to preservation solution [3]. This has important clinical implications, as these blebs may cause problems in biliary excretion as the blebs of sinusoidal endothelium cause disturbance of blood circulation. In human liver transplantation, ischaemic biliary complications with long preserved livers unrelated to arterial thrombosis or ABO incompatibility have been reported [21, 38]. Our results indicate that bleb formation on bile canaliculi may be a factor in these biliary complications.

The morphological changes in Kupffer cells look similar to the endothelial cells. Small blebs with high electron density and IMP redistribution are observed at 8 h and these cells are apparently more vulnerable to cold storage than hepatocytes. There are contradictory reports of the fate of the Kupffer cell, some report that it is activated [4, 34], while others consider it to be injured [2, 20]. Activation and injury may both occur.

Autophagosomes were fond in hepatocytes in this work, and have been formed within 15 min of perfusing the liver with an amino acid free solution [10]. They are also formed during hypoxia [15]. Autophagosomes are considered to originate from ribosome-free regions of rER [10] although SER [1], lysosomes [37] and Golgi-associated ER from which lysosomes form [30] are also proposed as origins. A sheet of ribosome-free rER invaginates and surrounds intracellular organelles and forms an autophagosome with double membranes. The inner membrane is then degraded and transformed into an autophagic vacuole [9, 10]. The function of the autophagosome is to rid the cell of "worn-out" organelles [14], but its physiological role during hypothermic preservation is not clear.

Acknowledgements The authors are indebted to Dr. Robert C. Harvey and Delin West for critically reviewing the manuscript and correcting the English.

References

1. Arstila AU, Trump BF (1969) Autophagocytosis: origin of membrane and hydrolytic enzymes. Virchows Arch [B] 2: 85–90
2. Belzer FO, May R, Berry MN, Phil D, Lee JC (1970) Short term preservation of porcine livers. J Surg Res 10: 55–61
3. Belzer FO, Southard JH, D'Alessandro AM, Knechtle SJ, Sollinger HW, Kalayoglu M (1993) Update on preservation of liver grafts. Transplant Proc 25: 2010–2011
4. Caldwell-Kenkel JC, Currin RT, Tanaka Y, Thurman RG, Lemasters JJ (1991) Kupffer cell activation and endothelial cell damage after storage of rat livers: effects of reperfusion. Hepatology 13: 83–95
5. Chiang J, Kowada M, Ames A, Wright RL, Majno G (1968) Cerebral ischemia. III. Vascular changes. Am J Physiol 52: 455–476

6. Coleman SE, Duggan J, Hackett RL (1976) Plasma membrane changes in freeze-fractured rat kidney cortex following renal ischemia. Lab Invest 35: 63–70
7. Derus BV, Behnke O (1980) Membrane structure of nonactivated and activated human blood platelets as revealed by freeze-fracture: evidence for particle redistribution during platelet contraction. J Cell Biol 87: 209–218
8. Donohoe JF, Venkatachalam MA, Bernard DB, Levinsky NG (1978) Tubular leakage and obstruction after renal ischemia: structural-functional correlations. Kidney Int 13: 208–222
9. Dunn WA (1990) Studies on the mechanisms of autophage: formation of the autophagic vacuole. J Cell Biol 110: 1935–1945
10. Dunn WA (1990) Studies on the mechanisms of autophagy: formation of the autophagic vacuole. J Cell Biol 110: 1923–1933
11. Duppel W, Dahl G (1976) Effect of phase transition on the distribution of membrane-associated particles in microsomes. Biochim Biophys Acta 426: 408–417
12. Elgsaeter A, Shotton DM, Branton D (1976) Intramembrane particle aggregation in erythrocyte ghosts. II. The influence of spectrin aggregation. Biochim Biophys Acta 426: 101–122
13. Farber JL, Martin JT, Kenneth R, Chien BA (1978) Irreversible ischemic cell injury: prevention by chlorpromazine of the aggregation of the intramembranous particles of rat liver plasma membranes. Am J Pathol 92: 713–732
14. Fawcett DW (1986) A textbook of histology, 11th edn. W.B. Saunders, Philadelphia
15. Glinsmann WH, Ericsson LE (1966) Observations on the subcellular organization of hepatic parenchymal cells. II. Evolution of reversible alterations induced by hypoxia. Lab Invest 15: 762–777
16. Gulian JM, Dalmasso C, Desmoulin F, Scheiner C, Cozzone PJ (1992) Twenth-four-hour hypothermic preservation of rat liver with Euro-Collins and UW solutions: a comparative evaluation by ^{31}NMR spectroscopy, biochemical assays, and light microscopy. Transplantation 54: 599–603
17. Herman B, Nieminen A, Gores GJ, Lemasters JJ (1988) Irreversible injury in anoxic hepatocytes precipitated by an abrupt increase in plasma membrane permeability. FASEB J 2: 146–151
18. Holloway CMB, Harvey PRC, Mullen JBM, Strasberg SM (1989) Evidence that cold preservation-induced microcirculatory injury in liver allografts is not mediated by oxygen-free radicals or cell swelling in the rat. Transplantation 48: 179–188
19. Holloway CMB, Harvey PRC, Strasberg SM (1990) Viability of sinusoidal lining cells in cold-preserved rat liver allografts. Transplantation 49: 225–229
20. Ikeda T, Yanaga K, Kishikawa K, Kakizoe S, Shimada M, Sugimachi K (1992) Ischemic injury in liver transplantation:difference in injury sites between warm and cold ischemia in rats. Hepatology 16: 454–461
21. Kadmon M, Bleyl J, Küppers B, Otto G, Herfarth C (1993) Biliary complications after prolonged University of Wisconsin preservation of liver allografts. Transplant Proc 25: 1651–1652
22. Lemasters JJ, Ji S, Thurman RG (1981) Centrilobular injury following hypoxia in isolated, perfused rat liver. Science 213: 661–663
23. Lemasters JJ, Stemkowski CJ, Ji S, Thurman RG (1983) Cell surface changes and enzyme release during hypoxia and reoxygenation in the isolated, perfused rat liver. J Cell Biol 97: 778–786
24. Lemasters JJ, DiGuiseppi J, Nieminen A, Herman B (1987) Blebbing, free Ca^{2+} and mitochondrial membrane potential preceding cell death in hepatocytes. Nature 325: 78–81
25. Majno G, Ames A, Chiang J, Wright RL (1967) No reflow after cerebral ischaemia. Lancet 2: 569–570
26. McKeown CMB, Edwards V, Philips MJ, Harvey PRC, Petrunka CN, Strasberg SM (1988) Sinusoidal lining cell damage: the critical injury in cold preservation of liver allografts in the rat. Transplantation 46: 178–191
27. Momii S, Koga A (1990) Time-related morphological changes in cold-stored rat livers: a comparison of Euro-Collins solution with UW solution. Transplantation 50: 745–750
28. Momii S, Koga A, Eguchi M, Fukuyama T (1989) Ultrastructural changes in rat liver sinusoids during storage in cold Euro-Collins solution. Virchows Arch [B] 57: 393–398
29. Myagkaya G, Veen HA, James J (1987) Ultrastructural changes in the rat liver during Euro-Collins storage, compared with hypothermic in vitro ischemia. Virchows Arch [B] 53: 176–182
30. Novikoff AB, Shin W-Y (1978) Endoplasmic reticulum and autophagy in rat hepatocytes. Proc Natl Acad Sci USA 75: 5039–5042
31. Okouchi Y, Tamaki T, Kozaki M (1991) Comparison of Na- and K-rich solutions in liver preservation for transplantation. Cryo Lett 12: 307–314
32. Okouchi Y, Tamaki T, Kozaki M (1992) The optimal temperature for hypothermic liver preservation in the rat. Transplantation 54: 1129–1130
33. Orci L, Perrelt A (1973) Membrane-associated particles: increase at sites of pinocytosis demonstrated by freeze-etching. Science 181: 868–869
34. Post S, Gonzalez A, Palma P, Rentsch M, Stiehl A, Menger MD (1992) Assessment of hepatic phagocytic activity by in vivo microscopy after liver transplantation in the rat. Hepatology 16: 803–809
35. Pringle MJ, Chapman D (1981) Biomembrane structure and effects of temperature. In: Morris GJ, Clarke GJ (eds) Effects of low temperatures on biological membranes. Academic Press, London, pp 21–37
36. Réz G, Meldolesi J (1980) Freeze-fracture of drug-induced autophagocytosis in the mouse exocrine pancreas. Lab Invest 43: 269–277
37. Saito T, Ogawa K (1974) Lysosomal changes in rat hepatic parenchymal cells after glucagon administration. Acta Histochem Cytochem 7: 1–18
38. Sanchez-Urdazpal L, Gores GJ, Ward EM, Maus TP, Wahlstrom HE, Moore SB, Wiesner RH, Krom AF (1992) Ischemic-type biliary complications after orthotopic liver transplantation. Hepatology 16: 49–53
39. Sasaki K (1988) A simple method to observe intracellular organelles with the scanning electron microscope. J Electron Microsc (Tokyo) 37: 171–173
40. Sasaki K, Ichikawa M (1993) The dynamics of intramembranous particles in the degradative pathways of the phagocytosed erythrocyte. Tissue Cell 25: 275–287
41. Sasaki K, Okouchi Y, Pabst R, Rothkötter H-J (1993) Three-dimensional detection of the expression of intercellular adhesion molecule-1 (ICAM-1) in the high endothelial venule (HEV) of the rat lymph node. Microsc Res Tech 25: 264–265
42. Soloff BL, Nagle AJ, Moss AJ, Henle KJ, Crawford JT (1987) Apoptosis induced by cold shock in vitro is dependent on cell growth phase. Biochem Biophys Res Commun 145: 876–883
43. Takei Y, Marzi I, Gao W, Gores GJ, Lemasters JJ, Thurman RG (1991) Leukocyte adhesion and cell death following orthotopic liver transplantation in the rat. Transplantation 51: 959–965
44. Wahlberg J, Southard JH, Belzer FO (1986) Development of a cold storage solution for pancreas preservation. Cryobiology 23: 477–482